Supplemental Material Figures S5 to S7, Smith and Edwards 2020, Improved status and trend estimates from the North American Breeding Bird Survey using a Bayesian hierarchical generalized additive model

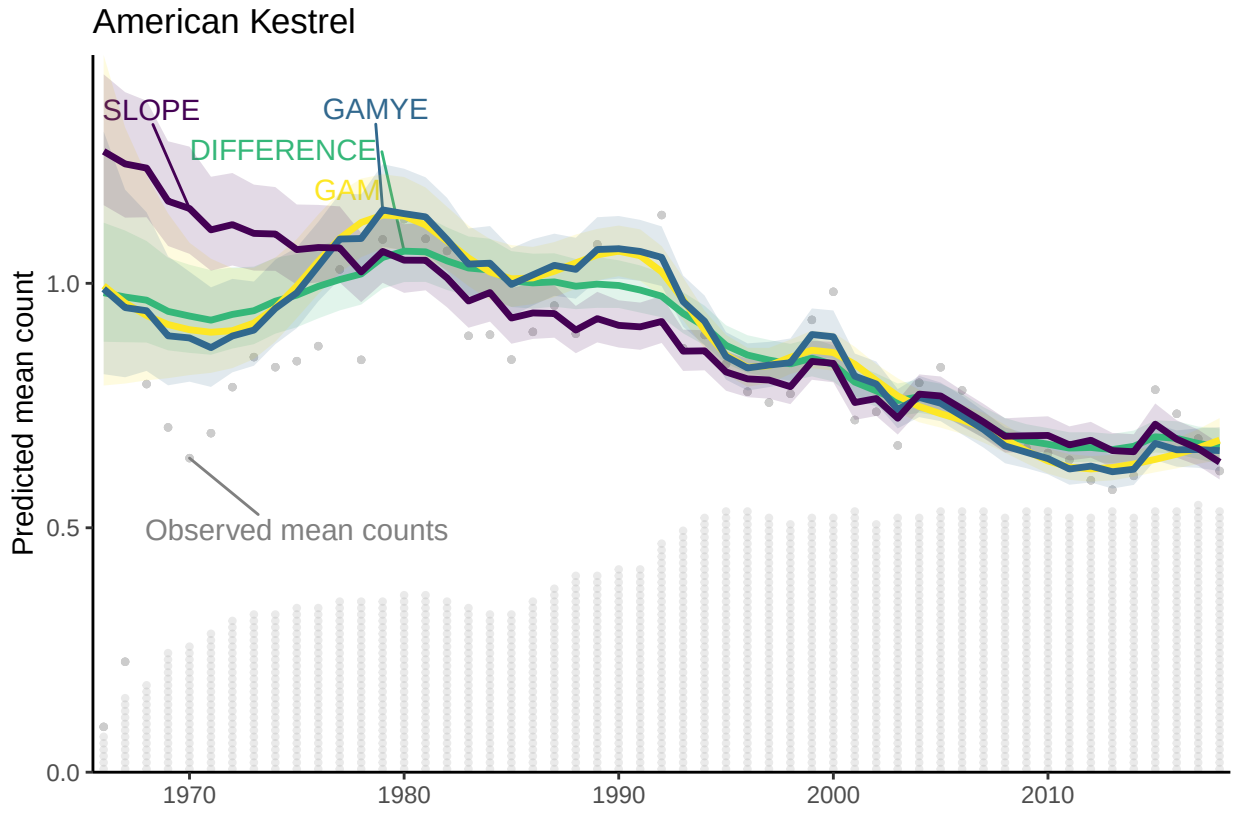

Figure 1: S5.A: Predicted survey-wide population trajectories from four models applied to the American Kestrel data from the BBS. The stacked dots along the x axis indicate the approximate number of BBS counts used in the model; each dot represents 50 counts.

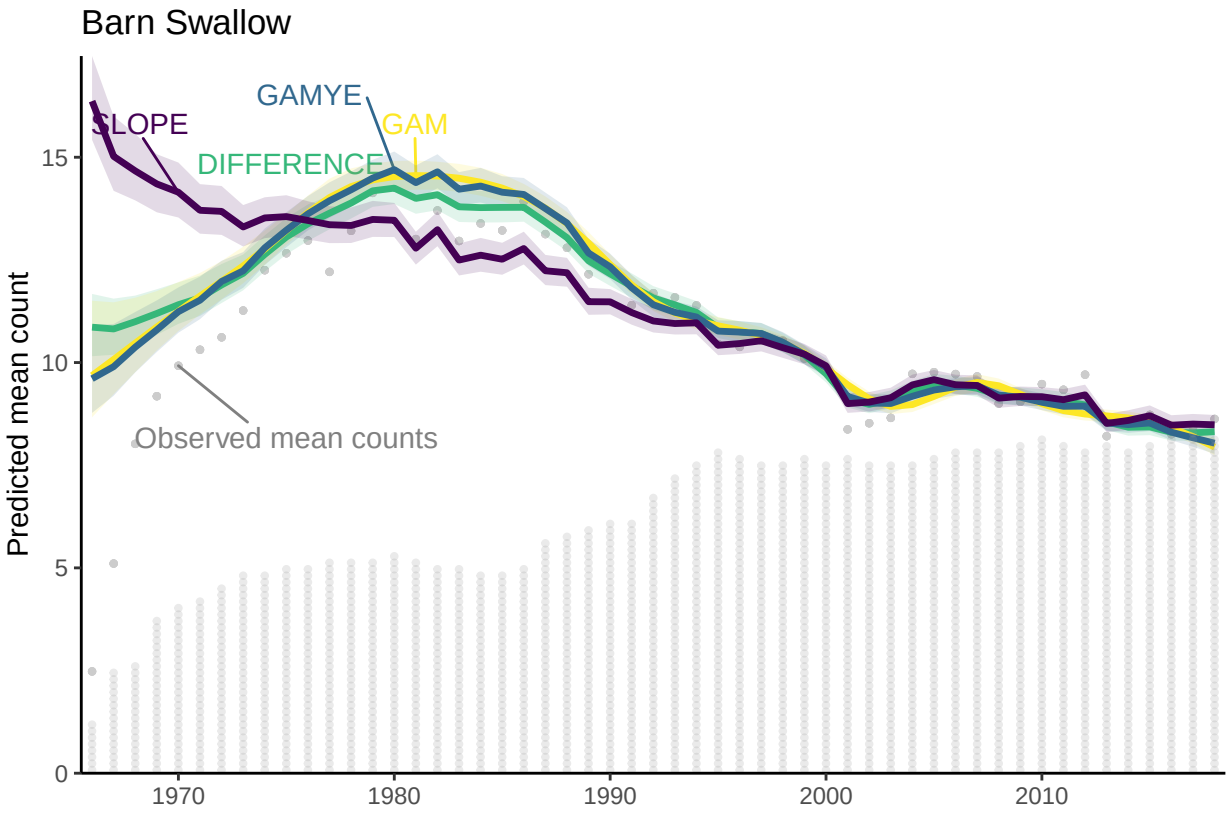

Figure 2: S5.B: Predicted survey-wide population trajectories from four models applied to the Barn Swallow data from the BBS. The stacked dots along the x axis indicate the approximate number of BBS counts used in the model; each dot represents 50 counts.

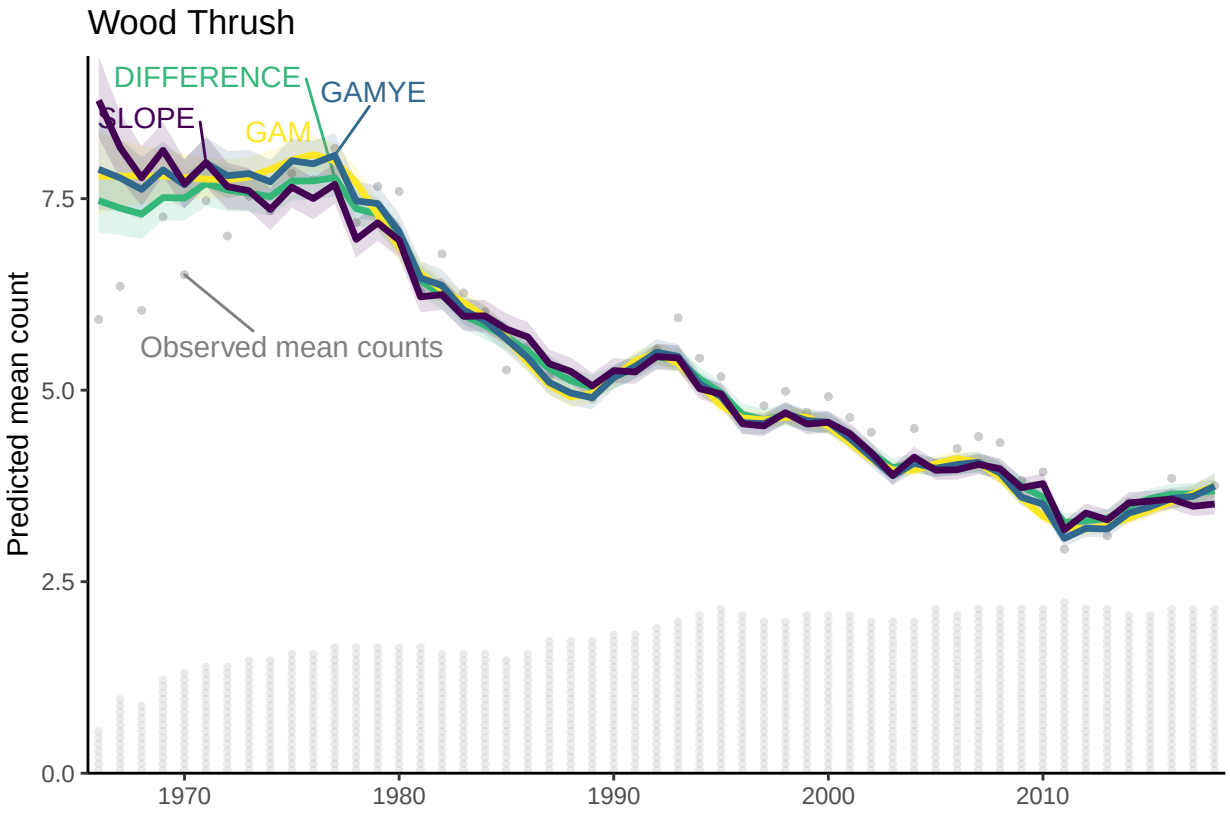

Figure 3: S5.C: Predicted survey-wide population trajectories from four models applied to the Wood Thrush data from the BBS. The stacked dots along the x axis indicate the approximate number of BBS counts used in the model; each dot represents 50 counts.

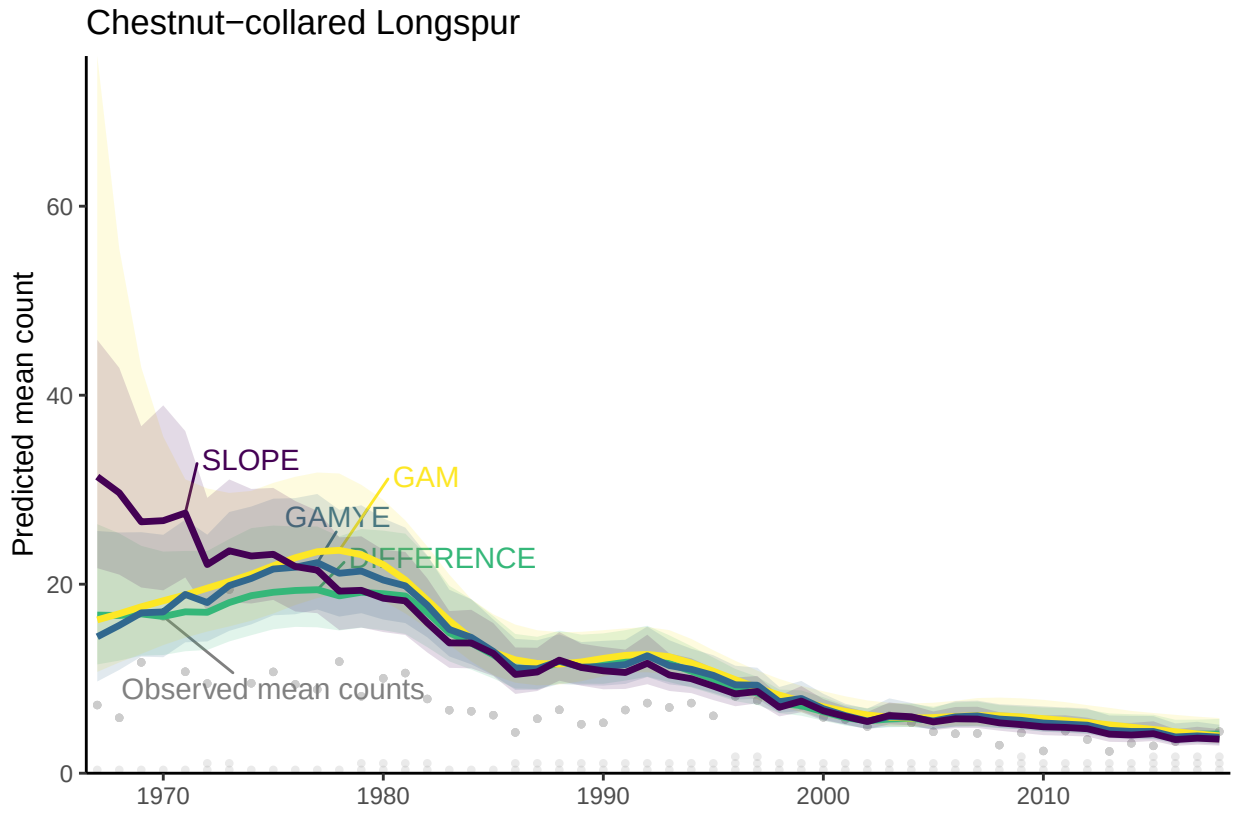

Figure 4: S5.D: Predicted survey-wide population trajectories from four models applied to the Chestnut-collared Longspur data from the BBS. The stacked dots along the x axis indicate the approximate number of BBS counts used in the model; each dot represents 50 counts.

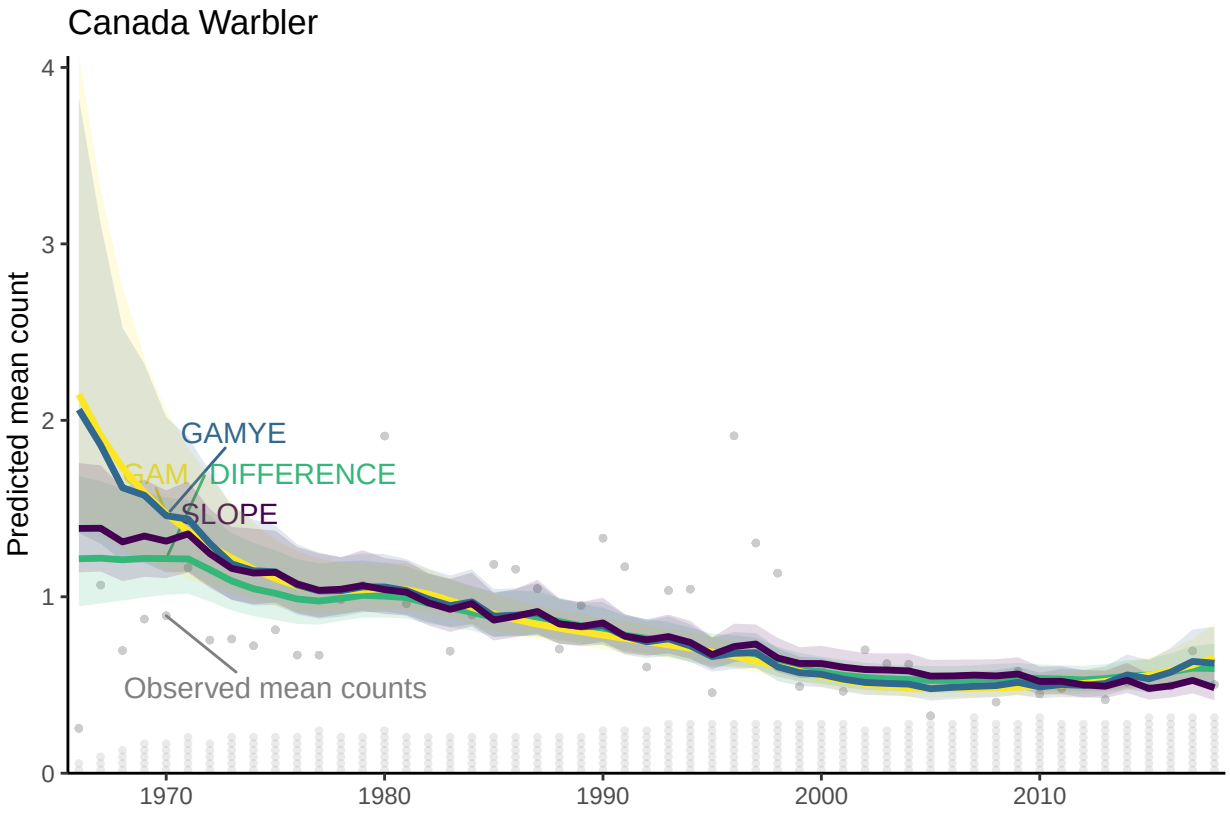

Figure 5: S5.E: Predicted survey-wide population trajectories from four models applied to the Canada Warbler data from the BBS. The stacked dots along the x axis indicate the approximate number of BBS counts used in the model; each dot represents 50 counts.

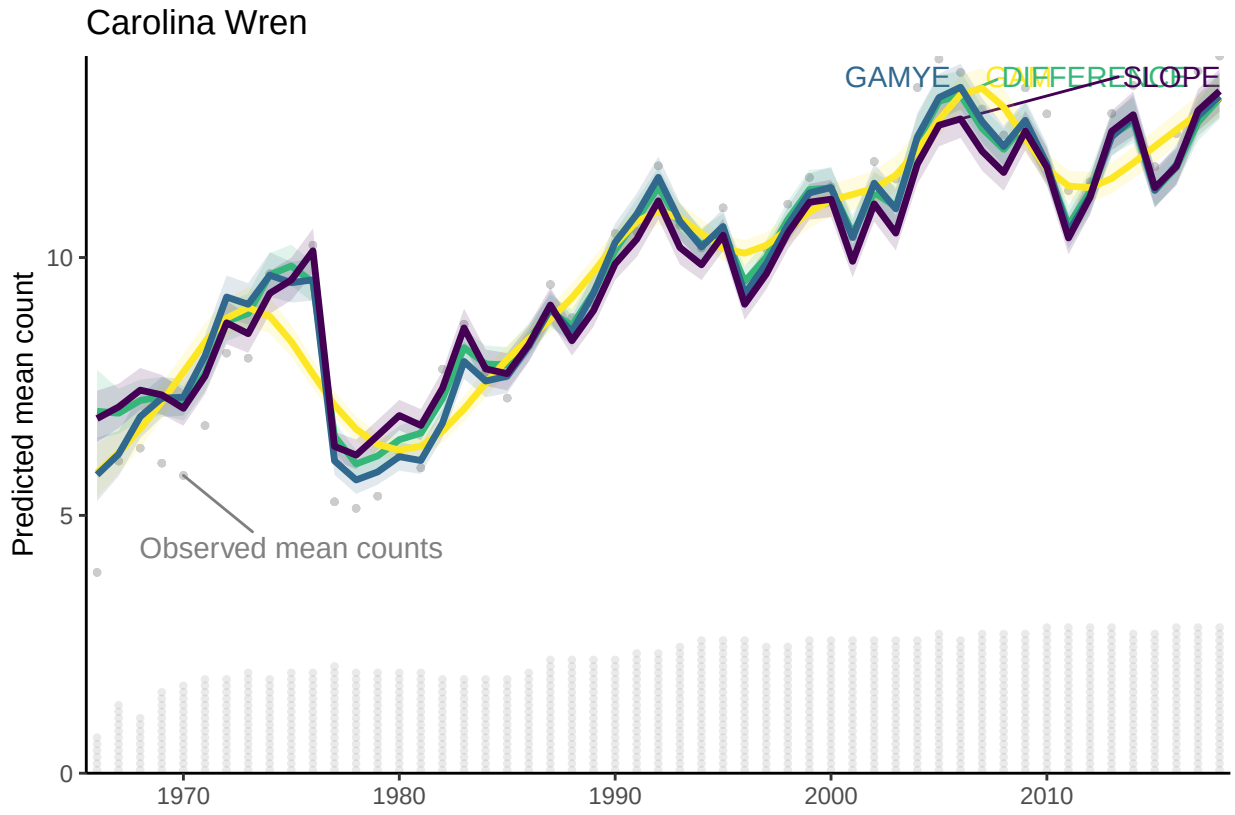

Figure 6: S5.F: Predicted survey-wide population trajectories from four models applied to the Carolina Wren data from the BBS. The stacked dots along the x axis indicate the approximate number of BBS counts used in the model; each dot represents 50 counts.

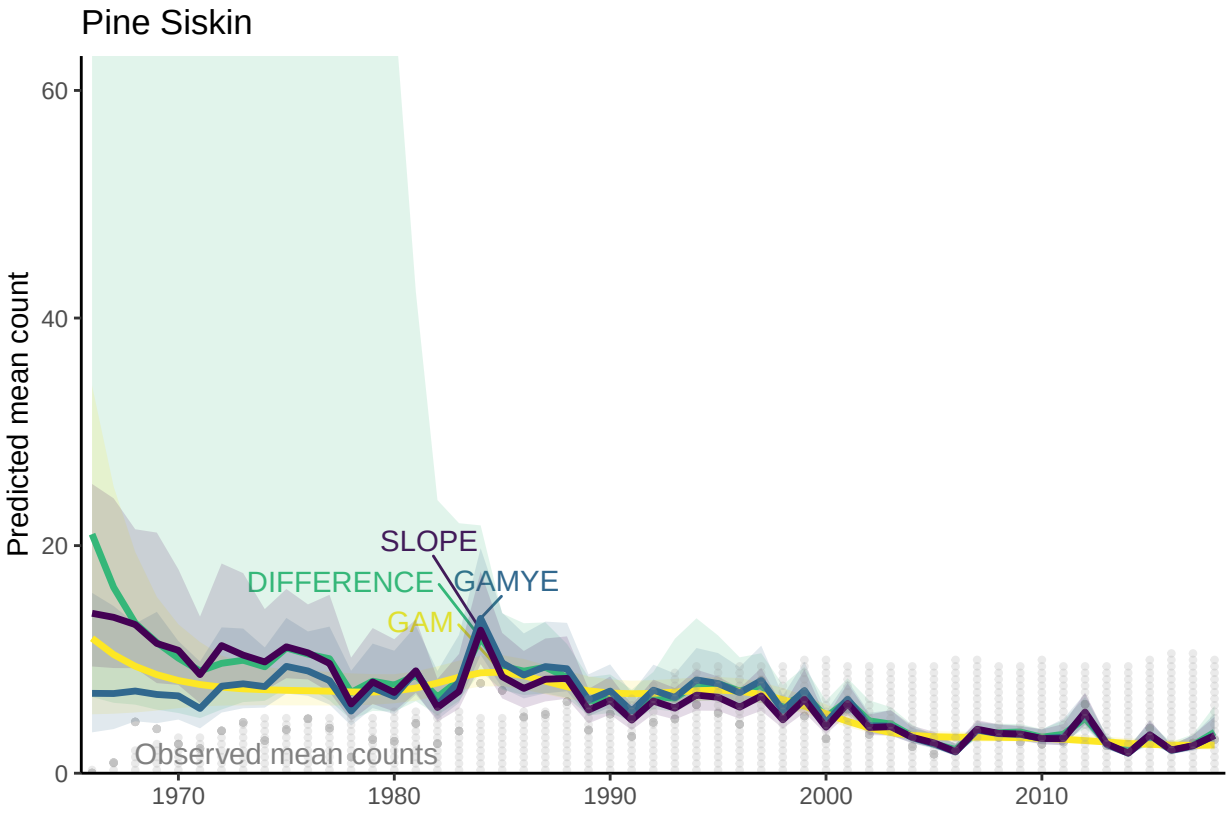

Figure 7: S5.G: Predicted survey-wide population trajectories from four models applied to the Pine Siskin data from the BBS. The stacked dots along the x axis indicate the approximate number of BBS counts used in the model; each dot represents 50 counts.

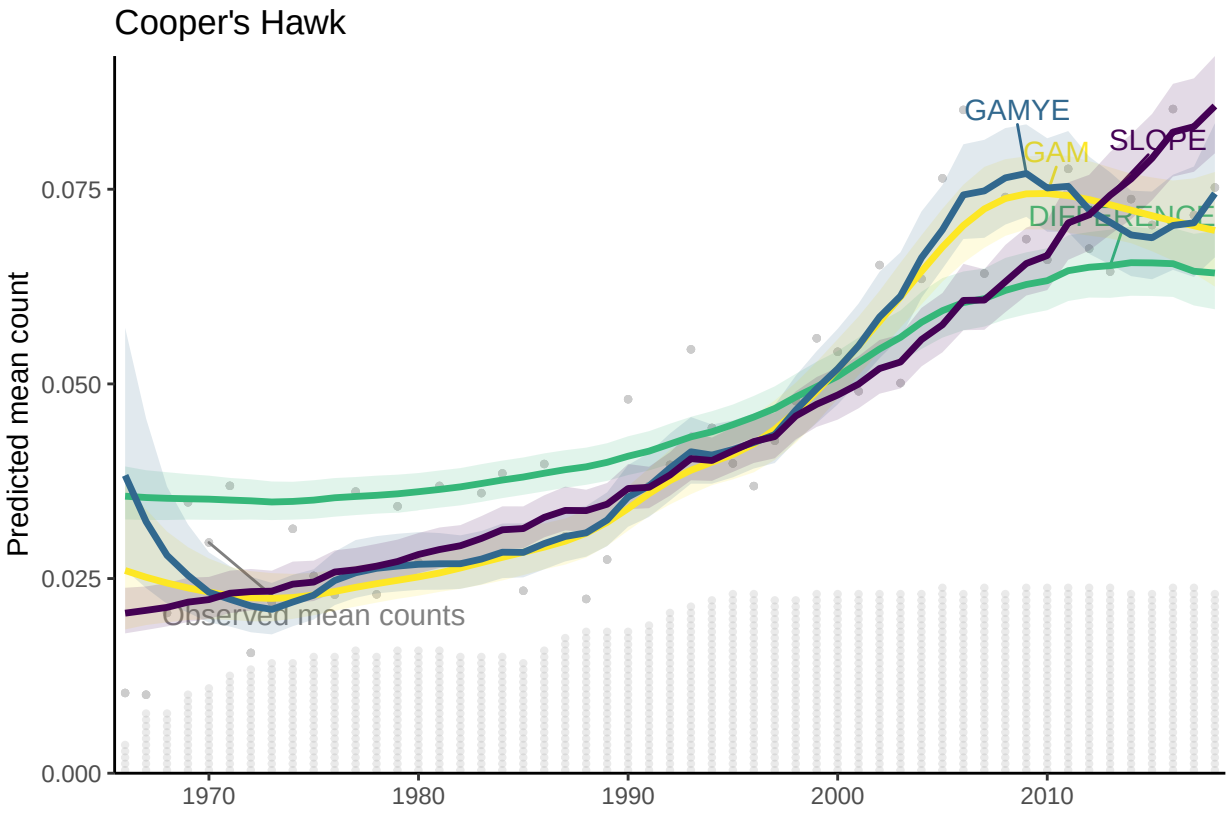

Figure 8: S5.H: Predicted survey-wide population trajectories from four models applied to the Cooper's Hawk data from the BBS. The stacked dots along the x axis indicate the approximate number of BBS counts used in the model; each dot represents 50 counts.

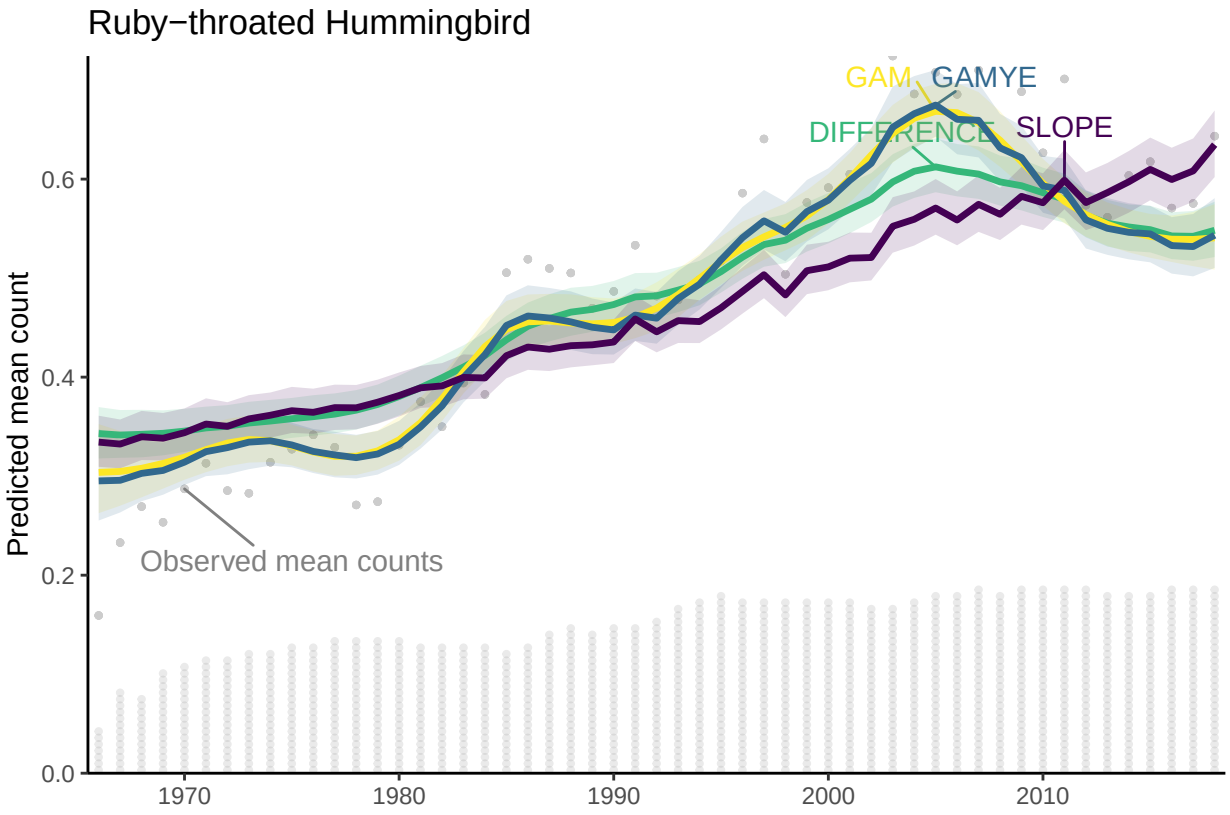

Figure 9: S5.I: Predicted survey-wide population trajectories from four models applied to the Ruby-throated Hummingbird data from the BBS. The stacked dots along the x axis indicate the approximate number of BBS counts used in the model; each dot represents 50 counts.

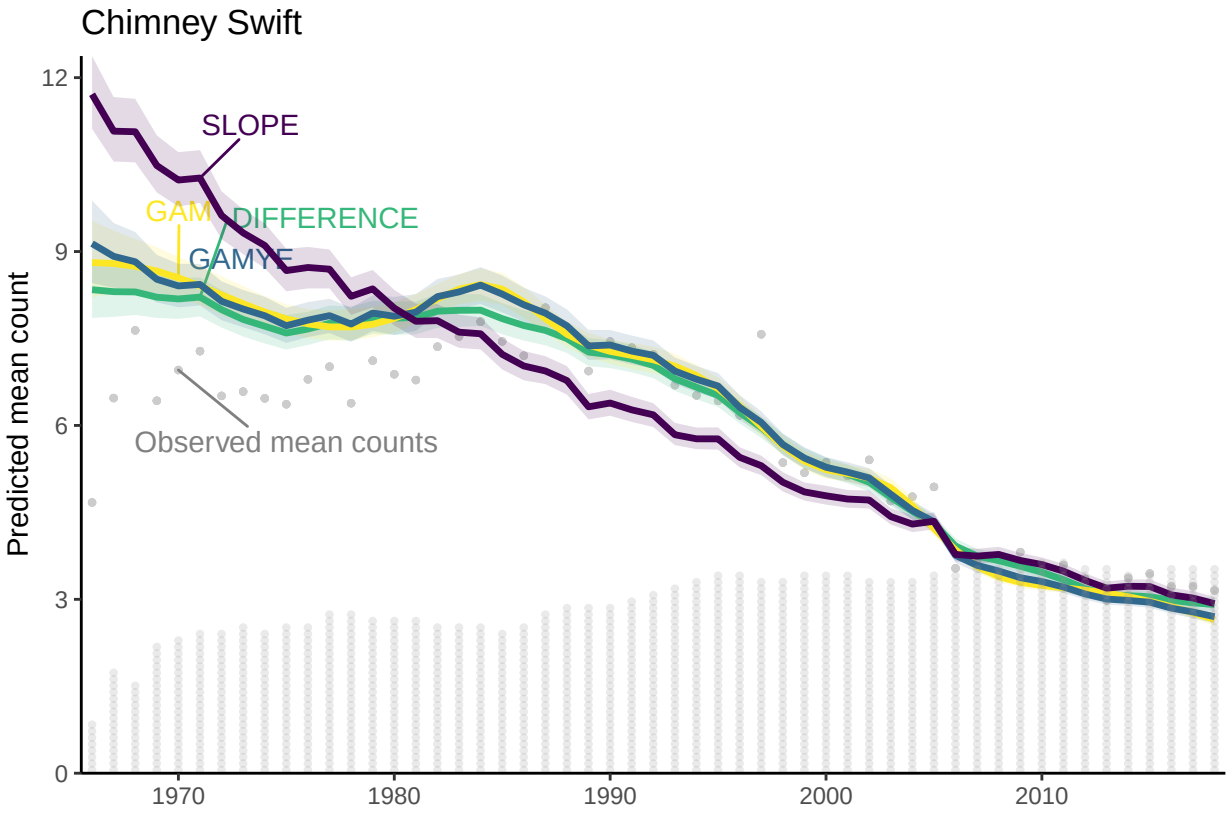

Figure 10: S5.J: Predicted survey-wide population trajectories from four models applied to the Chimney Swift data from the BBS. The stacked dots along the x axis indicate the approximate number of BBS counts used in the model; each dot represents 50 counts.

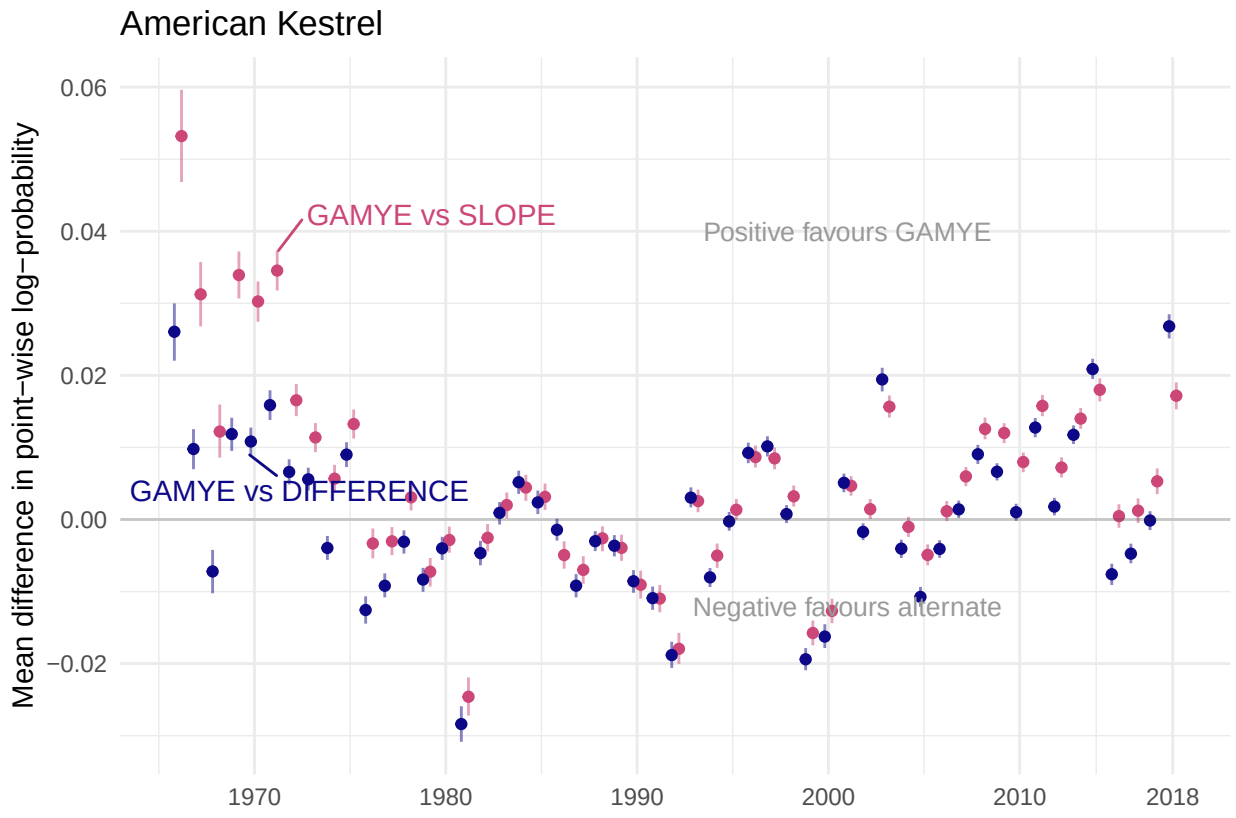

Figure 11: S6.A: Annual differences in predictive fit between the GAMYE and SLOPE (blue) and the GAMYE and DIFFERENCE model (red) for American Kestrel

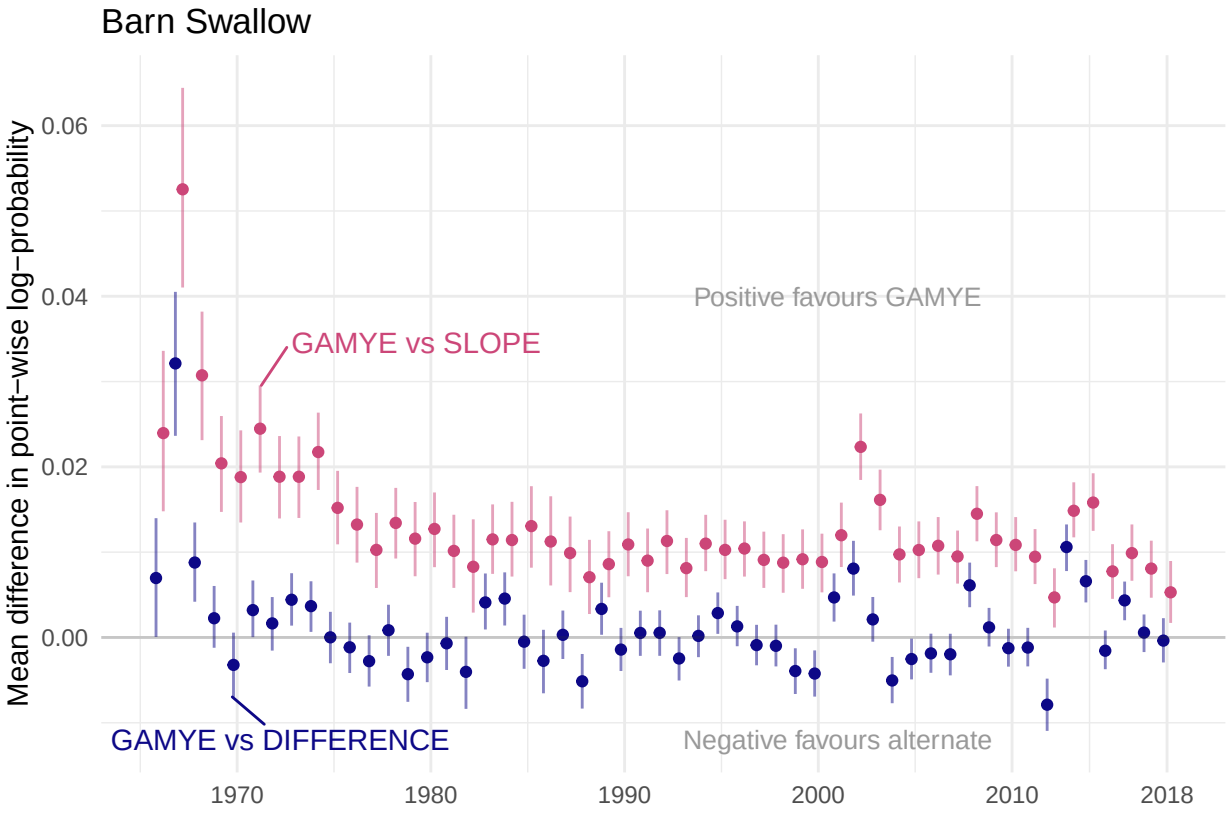

Figure 12: S6.B: Annual differences in predictive fit between the GAMYE and SLOPE (blue) and the GAMYE and DIFFERENCE model (red) for Barn Swallow

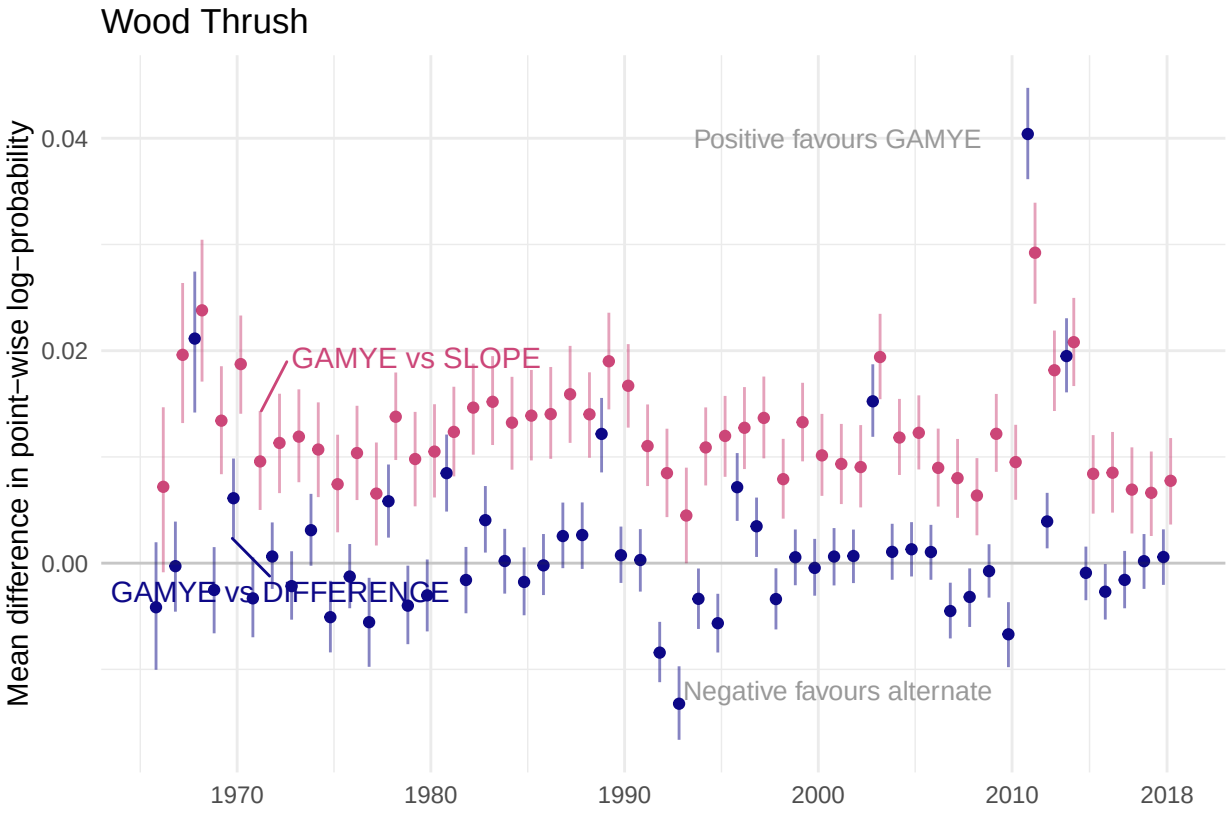

Figure 13: S6.C: Annual differences in predictive fit between the GAMYE and SLOPE (blue) and the GAMYE and DIFFERENCE model (red) for Wood Thrush

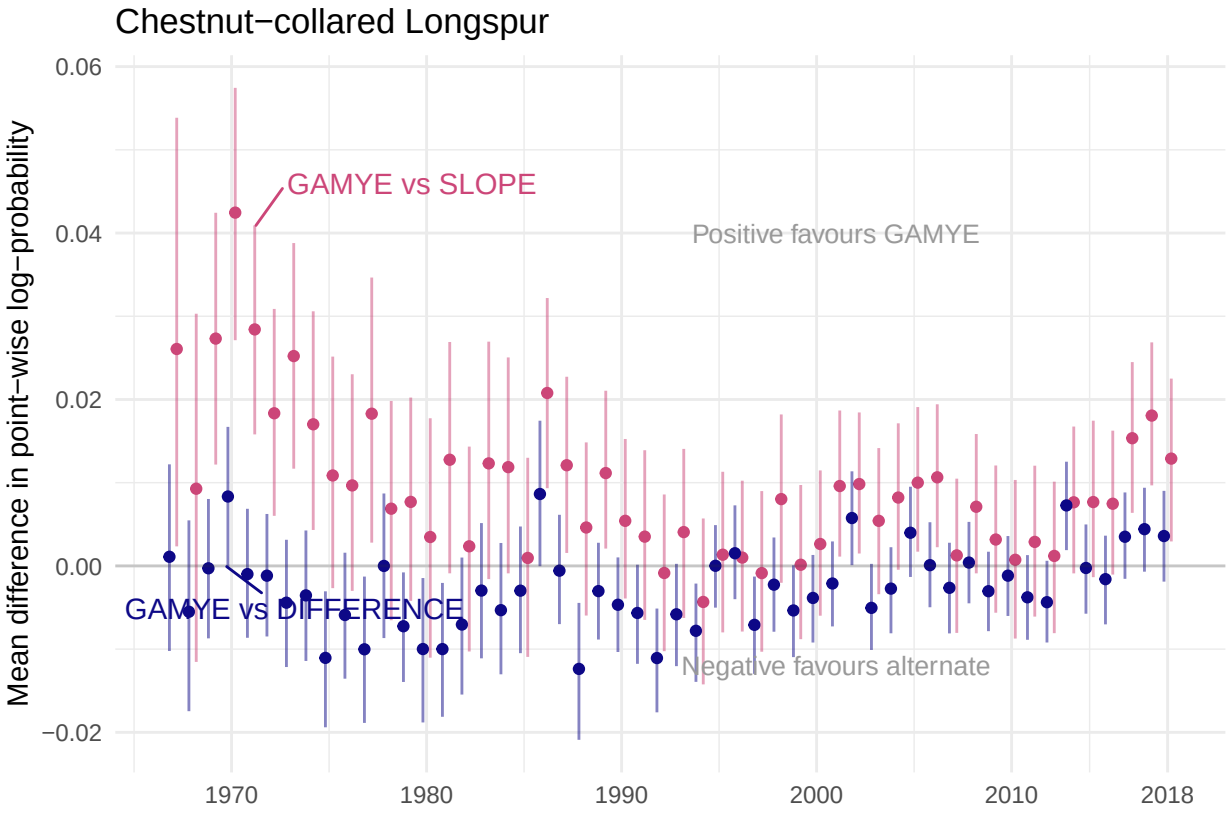

Figure 14: S6.D: Annual differences in predictive fit between the GAMYE and SLOPE (blue) and the GAMYE and DIFFERENCE model (red) for Chestnut-collared Longspur

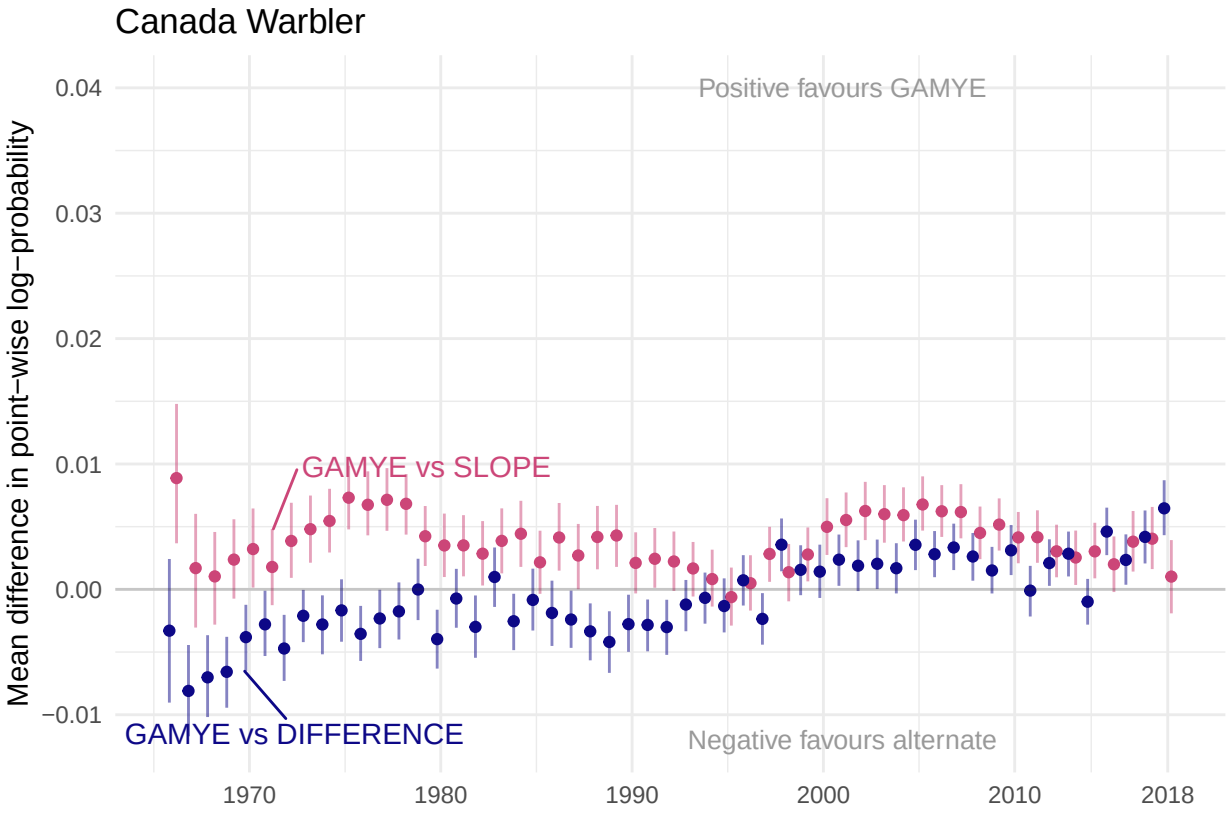

Figure 15: S6.E: Annual differences in predictive fit between the GAMYE and SLOPE (blue) and the GAMYE and DIFFERENCE model (red) for Canada Warbler

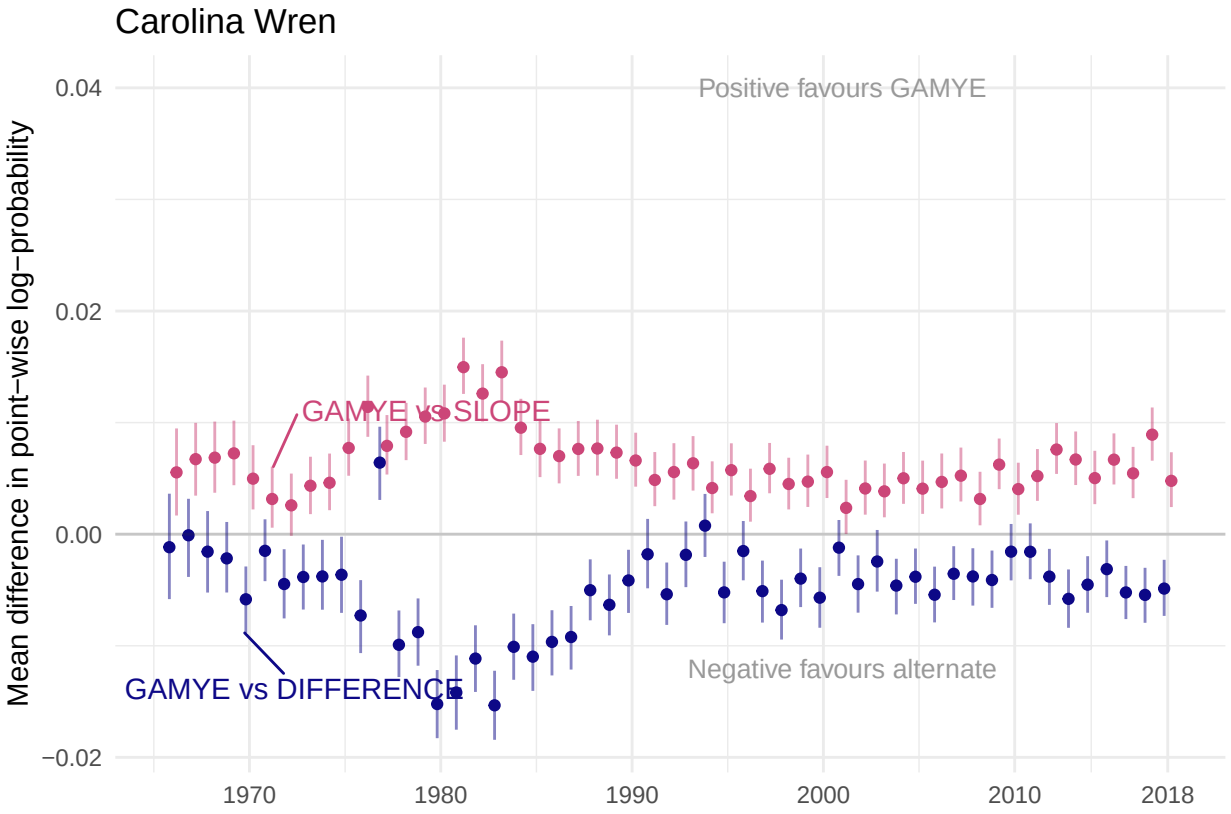

Figure 16: S6.F: Annual differences in predictive fit between the GAMYE and SLOPE (blue) and the GAMYE and DIFFERENCE model (red) for Carolina Wren

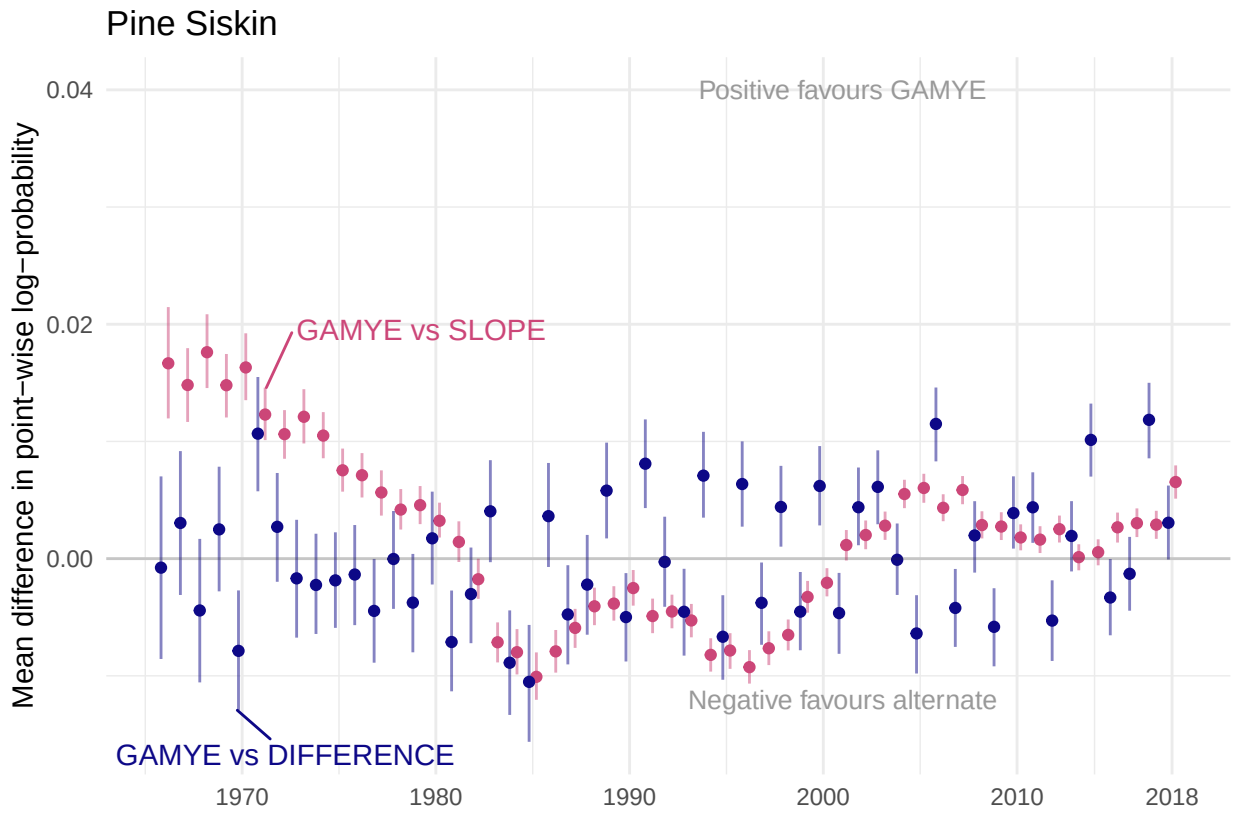

Figure 17: S6.G: Annual differences in predictive fit between the GAMYE and SLOPE (blue) and the GAMYE and DIFFERENCE model (red) for Pine Siskin

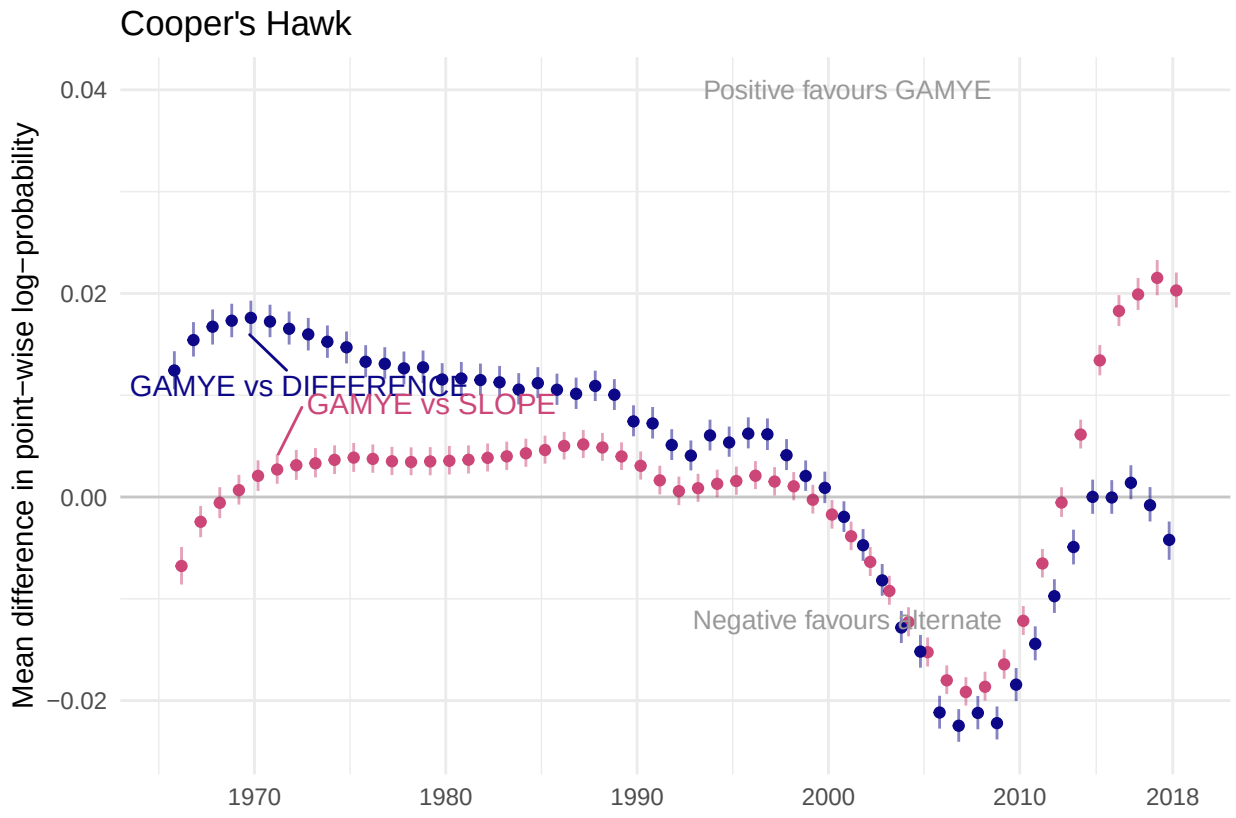

Figure 18: S6.H: Annual differences in predictive fit between the GAMYE and SLOPE (blue) and the GAMYE and DIFFERENCE model (red) for Cooper's Hawk

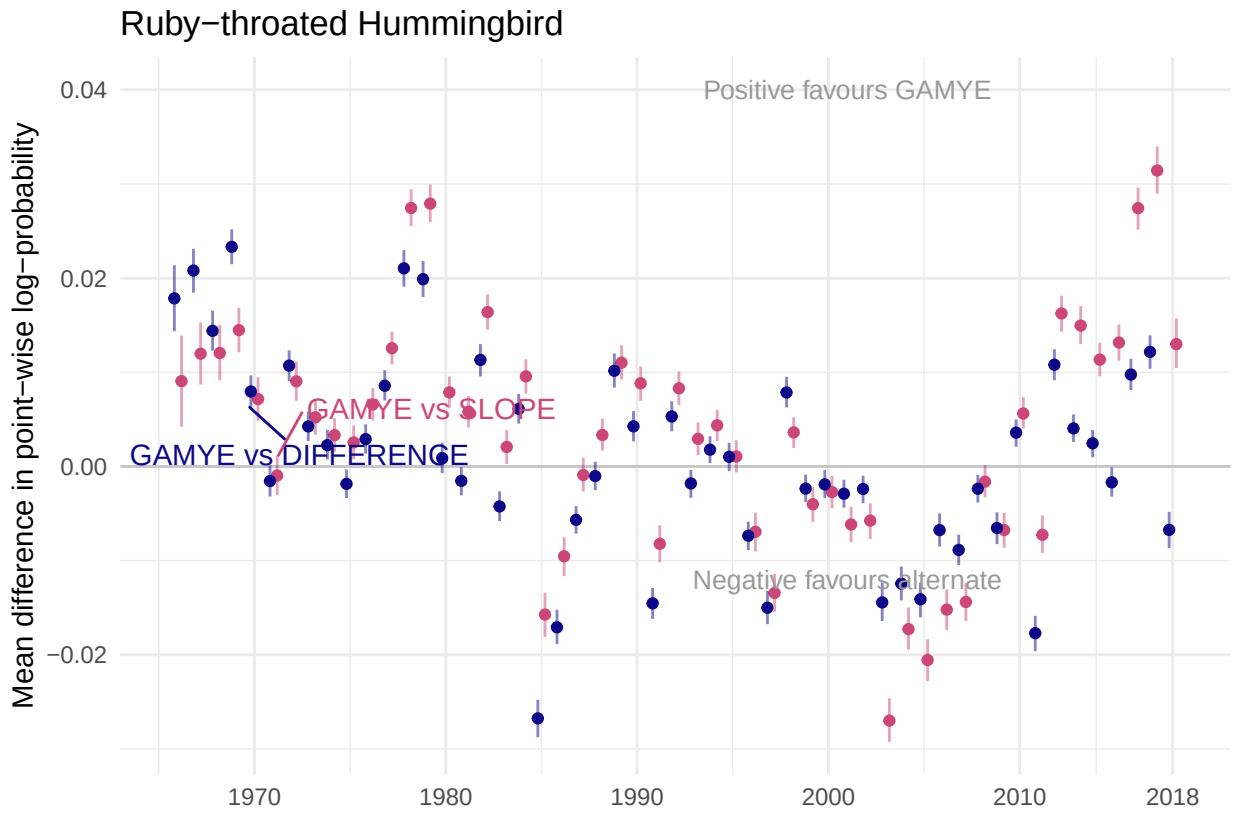

Figure 19: S6.I: Annual differences in predictive fit between the GAMYE and SLOPE (blue) and the GAMYE and DIFFERENCE model (red) for Ruby-throated Hummingbird

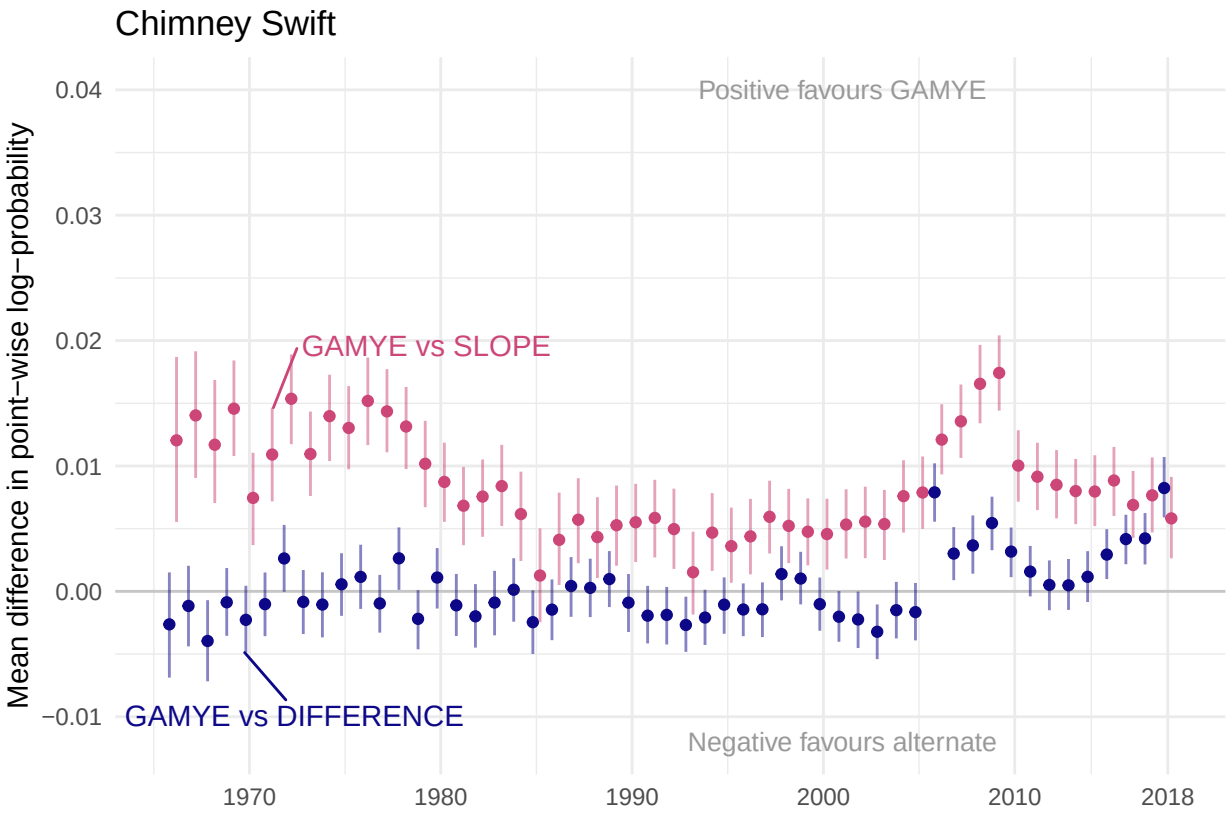

Figure 20: S6.J: Annual differences in predictive fit between the GAMYE and SLOPE (blue) and the GAMYE and DIFFERENCE model (red) for Chimney Swift

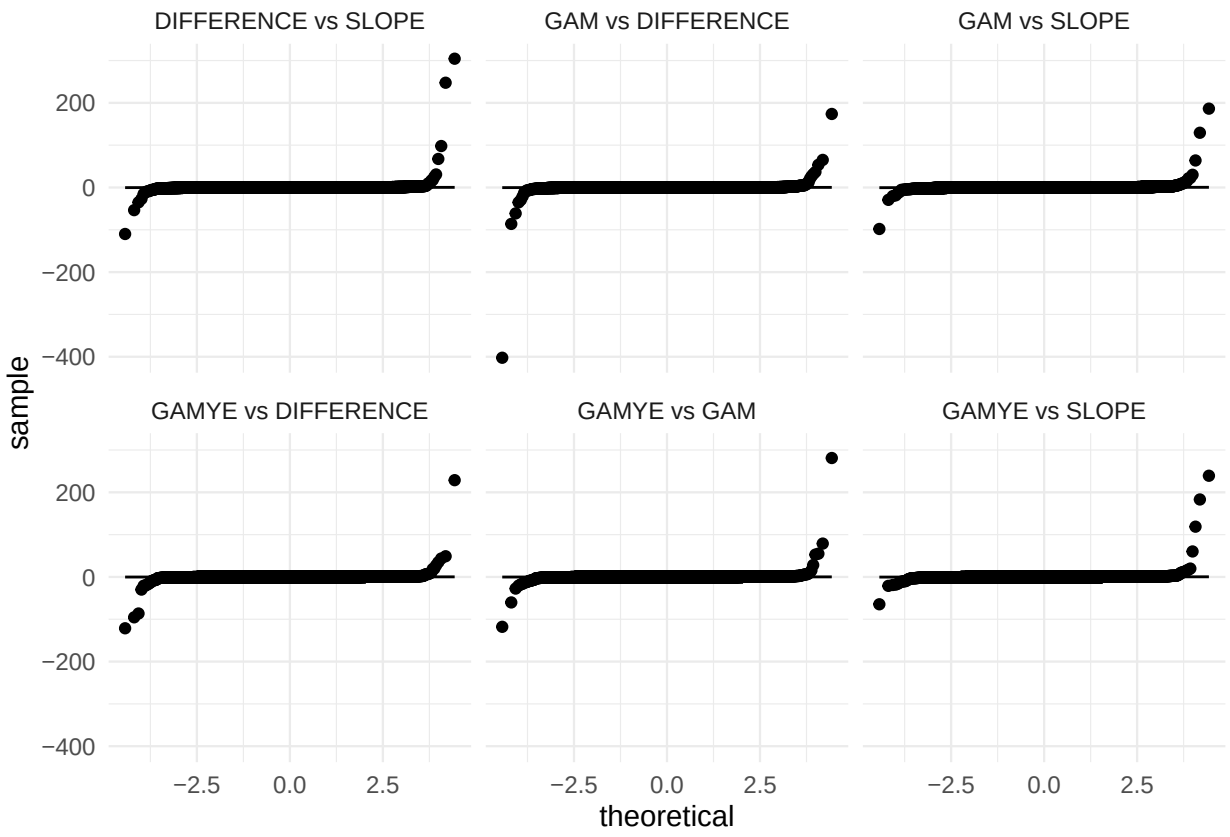

Figure 21: Figure S7: Normal qq plots for the differences in elpd between model pairs for Barn Swallow, demonstrating the non-normal distribution and the heavy tails better estimated using a t-distribution